A Novel Measurement Method for Performance Assessment of Hands-Free, XR-Based Human–Machine Interfaces

Leopoldo Angrisani, *Fellow, IEEE*, Mauro D'Arco, *Senior Member, IEEE*, Egidio De Benedetto, *Senior Member, IEEE*, Luigi Duraccio, *Member, IEEE*, Fabrizio Lo Regio, *Graduate Student Member, IEEE*, and Annarita Tedesco

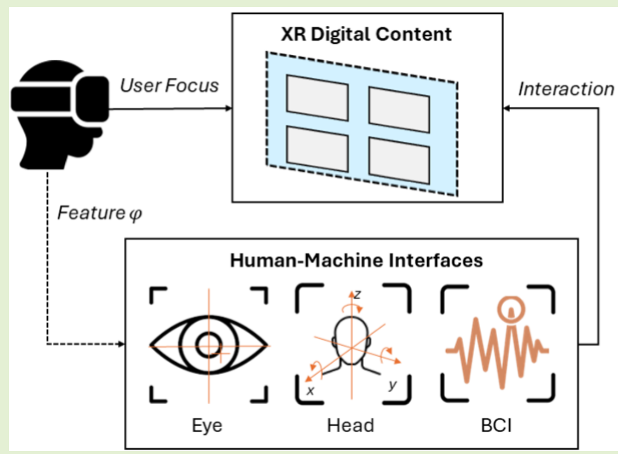

***Abstract*—This article presents an innovative measurement method for assessing the information transfer performance of hands-free human–machine interfaces (HMIs) based on extended reality (XR) technology. The proposed method primarily involves the design and implementation of a dedicated XR environment, which serves as a testbed for data acquisition. Following this, an experimental campaign is conducted, involving multiple acquisition cycles for different individuals. Finally, the proposed method enables extraction of two primary metrics, namely, selection accuracy and information transfer rate (ITR), indicative of the potential of the considered HMIs to transfer information. These metrics account for both intraindividual and interindividual variabilities within the HMIs, thus providing a metrologically sound assessment of performance. The proposed method is validated through a practical case study. Three NHMIs are considered: eye-tracking, head-tracking, and brain–computer interfaces (BCIs) based on steady-state visually evoked potentials (SSVEPs), as they allow hands-free interactions solely through visual observation. Without loss of generality, Microsoft HoloLens 2 and Unicorn Hybrid Black were used as XR and BCI platforms, respectively. The experimental findings obtained from eight healthy individuals allowed a comparative analysis of the performance of the three distinct HMIs, facilitating a better understanding of which interface might be more robust for a given application scenario. Overall, the proposed method represents a reliable performance assessment of innovative HMIs. This becomes increasingly significant considering the evolution of wearable HMIs and the current lack of comprehensive strategies for their characterization.**

***Index Terms*— Augmented reality (AR), brain–computer interfaces (BCIs), extended reality (XR), eye-tracking, head-tracking, human–machine interaction, human–machine interface (HMI), Industry 5.0, measurement, metrological characterization, virtual reality (VR).**

Manuscript received 9 July 2024; revised 31 July 2024; accepted 31 July 2024. Date of publication 21 August 2024; date of current version 2 October 2024. This work was supported by the Italian Ministry of University and Research (MUR) through the projects "Research and Innovation on Future Telecommunications Systems and Networks—RESTART," PNRR PE14 under Grant CUP E63C22002040007; "Made in Italy Circolare e Sostenibile," PNRR PE11 under Grant CUP E63C22002130007; and "A Multiscale Integrated Approach to the Study of the Nervous System in Health and Disease—MNESYS," PNRR M4C2 under Grant CUP E63C22002170007. The associate editor coordinating the review of this article and approving it for publication was Dr. Ing. Tai Fei. *(Corresponding author: Egidio De Benedetto.)*

This work involved human subjects or animals in its research. Approval of all ethical and experimental procedures and protocols was granted by Ethical Committee of Psychological Research of the University of Naples Federico II.

Please see the Acknowledgment section of this article for the author affiliations.

Digital Object Identifier 10.1109/JSEN.2024.3444472

I. Introduction

THE technological progress brought by the digital transition has significantly reshaped the dynamics between individuals and machines [1]. The adoption of human–machine interfaces (HMIs), which integrate hardware and software systems to enable communication between users and external devices, has indeed brought benefits in various application contexts, including industry [2], healthcare [3], and entertainment [4]. This communication is usually facilitated through the use of *tangible* devices, also named controllers, such as joypads, mice, or keyboards, characterized by undeniable reliability [5]. Nowadays, the transition to *Industry 5.0* further emphasizes human-centric approaches to digital technologies as one of its founding pillars, alongside sustainability and resilience [6]. As such, in the current *5.0* era, human centricity demands two fundamental requirements.

First, the adoption of innovative strategies that go beyond the use of controllers, such as hands-free solutions. This can be fulfilled through natural HMIs (NHMIs), wherein interactions are shaped by innate human actions or features [7]. This type of interaction is made possible by exploiting sensor systems, which sense users' actions with respect to the world around them. As such, NHMIs can be based on different principles. Among them, eye-tracking [8], head-tracking [9], and steady-state visually evoked potentials (SSVEPs) [10] have demonstrated great potential as they allow users to interact with external devices solely through visual observation.

The second requirement of human centricity is the wearability and portability of these NHMIs under consideration. Traditionally, experimental setups have imposed significant constraints on user mobility, often necessitating individuals to maintain a fixed position in front of cameras or LCD monitors. In this regard, extended reality (XR) has established itself as a cornerstone for NHMIs as it facilitates interactions by overlaying digital content onto the physical environment, in the case of augmented reality (AR) [11], or substituting it with an entirely simulated world perceived as real by the users, in the case of virtual reality (VR) [12].

To guarantee an effective and efficient interaction between users and the digital realm, in accordance with the *Industry 5.0* paradigm, these NHMIs must ensure that users' actions are rapidly and correctly recognized. Therefore, a performance assessment is necessary. This need becomes even more evident considering that despite NHMIs being recognized as a powerful means of human–machine interaction, to the authors' knowledge, XR manufacturers do not provide information regarding their true efficacy in information transfer, nor does the scientific literature offer a standardized method for obtaining such information. Such an effort is necessary to allow a better understanding of which HMIs are best suited, based on the available hardware and data processing strategies, to maximize information transfer.

Starting from these considerations, this study introduces a novel measurement method for evaluating the performance of hands-free, XR-based NHMIs. It involves designing and implementing a suitable XR environment, which serves as a testbed for the experimental campaign, which is carried out by considering multiple acquisition cycles for each participant. This approach allows for the extraction of two key metrics: selection accuracy and information transfer rate (ITR) [13], addressing both intraindividual and interindividual variabilities within the NHMI, thereby ensuring a metrologically robust performance assessment. The proposed method is validated through a practical case study with the three aforementioned NHMIs: 1) eye-tracking; 2) head-tracking; and 3) SSVEP. Without losing generality, Microsoft HoloLens 2 and Unicorn Hybrid Black were used as the XR and brain-computer interface (BCI) platforms, respectively.

This article is organized as follows. Section II provides a background of the considered NHMIs, i.e., eye-tracking, head-tracking, and SSVEP. In Section III, the proposed method for performance assessment is described. The implementation of the method in terms of hardware and software is shown in Section IV. The experimental setup and the obtained results are discussed in Section V. Finally, conclusions are drawn and the future work is outlined.

II. Background

NHMIs are characterized by low demand for physical effort (resulting in high usability and immersivity); hence, they are suitable even for individuals affected by physical disabilities [14] or lacking prior experience in XR-based HMI [7].

A useful categorization of XR-based NHMIs can be drawn between the below.

1) *Native NHMIs:* When they are implemented by users through the development of dedicated XR applications that use software libraries directly provided by the manufacturer of the XR platform [15].
2) *Integrated NHMIs:* When their implementation is made by means of external hardware and software systems integrated with the XR platform through application programming interfaces (APIs) [16].

Below follows a brief description of the three NHMIs under consideration.

A. Eye-Tracking NHMIs

Eye-tracking interfaces enable the recording and recognition of eye movements and features. Generally, the output of an eye-tracking device is an *eye-gaze* vector, which provides information about the direction the user is looking at [17].

With regards to XR technology, this process typically involves infrared (IR) stimulation and video-based processing [18]: an IR light irradiates the user's cornea, while a camera records the eye and identifies the difference between the position of the pupil and that of corneal reflection. In practical applications, the eye gaze thereby identified is used as an input for the selection of digital content. This allows its use as NHMI in the XR environment in different fields, including healthcare and safety in human–robot interaction [19].

Currently, eye-tracking NHMIs are native to many XR head-mounted displays (HMDs). The typical functional architecture is shown in Fig. 1(a). It consists of two main blocks, namely, an *XR application*, running on the XR HMD, which renders the digital content the user is interacting with, and an *eye-tracker*, which captures the features φ_e related to the movement of the user's eyes and provides, for each acquisition frame i, a set of coordinates (x_i, y_i), corresponding to the intersection points between the *eye gaze* vector and the plane on which the digital content is displayed. Feedback regarding the recognized selection made by the system can be displayed or used as input for actuators/commands, representing the *interaction* between the user and XR application.

B. Head-Tracking NHMIs

Head-tracking interfaces enable the estimation of the user's head position and orientation, combining them to provide information about the direction in which the user's head is pointing, described by the *head-gaze* vector [20], [21]. From a technological perspective, the process is based on the

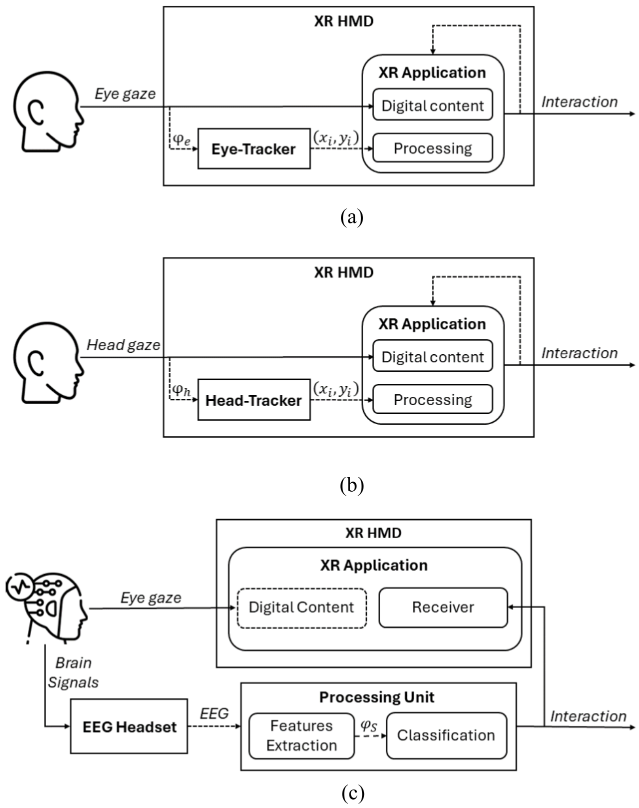

Fig. 1. Functional blocks of (a) eye-tracking, (b) head-tracking, and (c) SSVEP NHMIs.

analysis of data which can be collected by inertial measurement units (IMUs), and processed through robust algorithms and prediction techniques based on sensor fusion approaches such as simultaneous localization and mapping (SLAM) [22]. In practical applications [23], the identified head gaze serves as an input for the selection of digital content. It is worth mentioning that head-tracking NHMIs are advised to use cursors or other auditory/visual cues to provide users with confidence regarding their upcoming interactions [24].

Head-tracking NHMIs are currently native to all XR HMDs as *inside-out* or *outside-in* tracking systems [25], depending on whether internal or external units are used with the HMD, respectively.

The typical functional architecture is shown in Fig. 1(b). Similar to the eye-tracking interface, it includes the *XR application* block, along with a *head-tracker* which records the features φ_h related to user's head movements and provides coordinates (x_i, y_i) for each acquisition frame i, corresponding to the intersection points between the *head gaze* vector and the plane where the digital content is presented. Again, feedback regarding the recognized selection made by the system can be shown, representing the interaction between the user and XR application.

C. SSVEP-Based NHMIs

SSVEP-based NHMIs are a particular subset within the broader framework of BCIs. BCIs acquire neural signals from users and convert them into commands for external devices [26]. Among the main neural signal recording techniques in BCI, electroencephalography (EEG) allows noninvasiveness, wearability, and contained costs with respect to alternatives based on functional magnetic resonance (fMRI), magnetoencephalography (MEG), or near-infrared spectroscopy (NIRS) [27], [28]. In recent years, SSVEPs have garnered interest, emerging as some of the highest performing BCI systems [29], [30]. SSVEPs are induced within the primary visual cortex upon exposure to a flickering visual stimulus. The physiological brain response typically emerges with a latency spanning 80–160 ms [31]. It manifests as a sinusoidal-like waveform, showing the same frequency of the observed stimulus, and often higher harmonics [32]. Stimulus frequencies usually span from 1 to 100 Hz [33].

In practical applications, stimuli at different frequencies are typically associated with distinct commands/actuators selectable by the user. Consequently, SSVEP-based NHMIs enable users to choose the desired target by directing their *gaze* toward the corresponding flickering stimulus.

Recently, novel approaches leveraging XR HMDs for the rendering of the flickering stimuli have emerged as promising strategies to enhance portability, immersivity, and engagement in BCI applications with respect to traditional setups based on LCDs [13], thus facilitating the development of SSVEP-based NHMIs across diverse application contexts [34], [35], [36]. This allows considering BCIs based on SSVEPs and XR as a powerful integrated NHMI.

The typical functional architecture is shown in Fig. 1(c). Similar to eye-tracking and head-tracking NHMIs, it includes an XR HMD hosting an *XR application* responsible for rendering digital content, wherein each selectable icon flickers at a known frequency. An *EEG headset* captures the user EEG signal and transmits it to a *processing unit*, which can be integrated within either the XR HMD itself or an external unit. The processing unit extracts the relevant features φ_S from the EEG signal and provides a *classification*. Successful classification occurs when the output of the classifier matches the visual stimulus observed by the user. As an integrated NHMI, the XR application includes a *receiver* software module to retrieve the classifier output pertaining to the *interaction* between the user and the digital content.

III. Proposed Method

This section addresses the description of the proposed method for performance assessment of eye-tracking, head-tracking, and SSVEPs as NHMIs in XR environment.

The first step of this method requires the design of an XR environment, which serves as a testbed for the extraction of suitable metrics to assess the information transfer performance of the NHMIs under consideration.

A. Design of the XR Environment

The XR environment comprises a total of N_T icons, each of equal size and uniformly distributed within the field of view (FoV) of the XR HMD (x-y plane), positioned at an appropriate projected distance z from the user's perspective along the z-axis. The task design is described as follows.

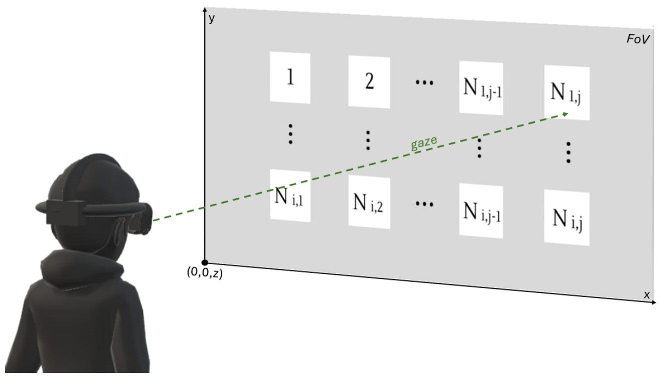

Fig. 2. Conceptual design of the XR environment as seen by the user.

1) Once the user wears the XR HMD, a visual cue appears at the center of each icon, one at a time in random order, to indicate which icon the user should gaze at for a certain acquisition time T. A brief rest interval is provided between each cue and the next one. The choice of randomizing visual cues was made to mitigate potential bias phenomena.
2) Once the visual cue has appeared on all N_T icons, one acquisition cycle is completed.
3) This procedure is repeated for C cycles for each of S individuals participating in the experiment and for each of the three NHMIs separately.

Overall, the XR environment and the experimental conditions remain consistent across all the three NHMIs. The unique difference lies in the SSVEP-based NHMI scenario, where each icon flickers at a known and fixed frequency f_{N_T} to elicit SSVEPs in the users.

For the sake of clarity, a sketch of the user view of the XR environment is shown in Fig. 2.

B. Performance Assessment

The performance of the three considered NHMIs is evaluated based on two metrics of interest, namely, selection accuracy (A) and ITR, which represent the most suitable metrics for understanding the efficiency of HMIs in information transmission [13].

The selection accuracy (A) is defined as the ratio between the number N_C of icons correctly selected by the HMI under test and the total number of icons N_T the user was asked to select during a single cycle

$$A = \frac{N_C}{N_T} \cdot 100. \tag{1}$$

On the other hand, the ITR represents a comprehensive indication of the amount of information conveyed by the HMI under test [13] and is expressed in bit/min. ITR considers the normalized selection accuracy p in the range [0, 1], the number of icons N_T that can be selected during a single cycle, and the acquisition time T (s)

$$\mathrm{ITR} = \left[\log_2(N_T) + p \cdot \log_2(p) + (1-p) \cdot \log_2\left(\frac{1-p}{N_T - 1}\right)\right] \times \frac{60}{T}. \tag{2}$$

To extract intra- and interindividual information from data acquisition, for each NHMI, the following pipeline was used.

1) First, selection accuracy values $A_{c,s}$ are extracted for each of the $c = 1, 2, \ldots, C$ cycles and for each of the $s = 1, 2, \ldots, S$ individuals involved in the experiments.
2) Then, the assessment of the mean selection accuracy $m(A)_s$ across the cycles and type-A evaluation of the uncertainty $u_A(A)_s$ is carried out [37].
3) Starting from $m(A)_s$, the corresponding mean ITR across the cycles $m(\mathrm{ITR})_s$ can be obtained through (2).
4) Evaluation of the standard uncertainty of the ITR $u(\mathrm{ITR})_s$ is conducted using $u_A(A)_s$ and exploiting the law of propagation of uncertainty (LPU) [37] assuming the quantities N_T and T without uncertainty as fixed during the design stage.

As such, each individual is associated with their own mean selection accuracy $m(A)_s$ and $m(\mathrm{ITR})_s$, along with the corresponding standard uncertainties $u(A)_s$ and $u(\mathrm{ITR})_s$ which represent the intraindividual variability of these metrics.

5) By averaging the selection accuracy and ITR across the individuals, it is possible to obtain an interindividual mean selection accuracy $\overline{m}(A)$ along with an interindividual selection accuracy $\overline{u}(A)$ obtained by means of LPU.
6) Finally, starting from $\overline{m}(A)$ and $\overline{u}(A)$, it is possible to evaluate the interindividual mean ITR $\overline{m}(\mathrm{ITR})$ through (2) along with an interindividual standard uncertainty $\overline{m}(\mathrm{ITR})$ obtained through LPU.

Overall, analyzing intraindividual variability allows for the assessment of individual consistency across repeated trials with the same NHMI. Hence, it can be associated with the concept of repeatability [37] Conversely, information on interindividual variability enables the evaluation of the results across different individuals using the same NHMI. In this framework, it can be associated with the definition of reproducibility [37].

IV. Implementation

Without losing generalization, this section describes the practical scenario considered to describe the application of the proposed method.

A. Hardware

The proposed method was implemented and tested using Microsoft HoloLens 2 [38], Unicorn Hybrid Black [39], and a high-performance processing unit as experimental platforms.

1) HoloLens 2 is a stand-alone, optical see-through XR HMD. It is equipped with a 60-Hz display and a 52° diagonal FOV. With reference to Fig. 1, it is the XR HMD chosen for the three NHMIs to render the digital content. It natively provides both eye-tracking and head-tracking NHMIs, enabled by means of a sensor apparatus consisting of IR illuminators and cameras for eye-tracking, as well as IMU and depth sensors for head-tracking. The integration with Unicorn Hybrid Black and processing unit to develop the SSVEP-based NHMI is made possible by Wi-Fi 5 and Bluetooth 5.0 modules.

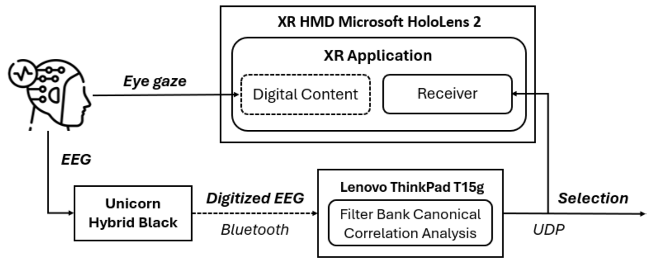

Fig. 3. Hardware diagram of the integrated SSVEP-based NHMI.

2) Unicorn Hybrid Black is a wearable, eight-channel EEG acquisition system. It is endowed with hybrid electrodes for dry or wet recordings, and it digitizes data with 250-sps sampling rate and 24-bit resolution. According to Fig. 1, it is the EEG headset chosen for the SSVEP-based NHMI. Through a Bluetooth 2.1 module and dedicated APIs, the EEG signals can be sent in real-time to external processing units [see Fig. 1(c)].
3) The selected processing unit to develop the SSVEP-based NHMI [see Fig. 1(c)] was a Lenovo ThinkPad T15g. It features an Intel Core i7-10750H CPU and 32 GB of RAM. The Bluetooth 5.1 module enables the reception of EEG data from the Unicorn Hybrid Black device, which are then processed using the dedicated Unicorn API. Subsequently, the results of the processing are transmitted to HoloLens 2 via UDP protocol.

While the HoloLens 2 device alone is sufficient for implementing the eye- and head-tracking NHMIs, the implementation of the SSVEP-based NHMI is illustrated in Fig. 3.

B. Development of the XR Environment

The XR environment was developed by means of the game engine Unity, the mixed reality toolkit (MRTK), and Visual Studio environment. Following the design sketched in Fig. 2, it consists of a grid of $N_T = 8$ squares sized 0.10×0.10 m, arranged in $i = 2$ rows and $j = 4$ columns, uniformly interspaced within the $x - y$ plane and projected at a distance z of 1.00 m from the user's view. The duration of the cue was set to 2.0 s, while the acquisition time T was chosen to be 1.5 s. In addition, a rest period of 2.0 s was established before the next cue. The number C of cycles was set equal to 5. Both the size of the objects and the time duration of the selection are compatible with the most recent AR scenarios and fixation times [40], [41], respectively.

With regard to eye- and head-tracking NHMIs, the squares were rendered in white color. Instead, regarding the SSVEP–BCI interface, during the acquisition time T, the squares flickered in grayscale following a sampled sinusoidal approach [13]. The chosen frequencies f_{N_T} were from 8 to 15 Hz with a 1-Hz span. This frequency band was chosen to ensure the maximum signal-to-noise ratio [13]. These frequencies were assigned clockwise starting from the top-left square. The phases ϕ were chosen to be equal to $-\pi/2$ for all the squares, ensuring they flickered starting from the same grayscale color.

C. Processing Strategy

With regard to both eye- and head-tracking NHMIs, data are acquired and processed using the *IMixedRealityEyeGazeProvider* library. This library enables the recognition of eye-gaze and head-gaze during the acquisition time T. The square on which the cue appeared will result as correctly observed if, for each frame f of the acquisition time, the coordinate vectors (x_f, y_f) described in Section II are located within that square.

Instead, regarding the SSVEP-based NHMI, EEG data are processed in Simulink environment using the Unicorn API. The SSVEP recognition is carried out using the filter-bank canonical correlation analysis (FBCCA) [42], a time-domain classification algorithm which is recognized as the state-of-the-art technique for SSVEP classification [13]. It combines canonical correlation analysis (CCA) with filter banks, enabling the exploration of correlations between different frequency components of multivariate data. By decomposing EEG signals into frequency subbands and subsequently performing CCA, this technique facilitates the identification of relationships between flickering stimuli and the resulting EEG signals. As such, the square on which the cue appeared will result as correctly classified if the frequency resulting from FBCCA corresponds to the flickering frequency of that square. The communication between the processing unit and the XR HMD is made via UDP protocol.

V. Experimental Results

A. Experimental Campaign and Results

The experimental campaign involved eight healthy individuals, age 22–29 years, balanced by sex, with normal and corrected-to-normal vision. Four participants had previous experience with XR HMDs, and among them, two individuals had previous experience in SSVEP-based NHMIs. The study was approved by the Ethical Committee of Psychological Research of the University of Naples Federico II, and all the individuals provided written informed consent before starting the experiments. The experiments were conducted in a dimly lit room, where individuals were seated, facing a wall approximately 2-m distant. Four wet electrodes, placed in *Pz*, *PO7*, *Oz*, and *PO8* positions, according to the 10–20 International System [13] were used. Finally, the individuals were instructed on the task to be performed. For each NHMI, all the individuals completed the $C = 5$ cycles, with each cycle involving the observation of $N_T = 8$ squares through the cue-guided selection.

The results in terms of selection accuracy (expressed as a percentage) and ITR (expressed in bit/min) for the three developed NHMIs are summarized in Tables I and II for each individual and cycle, along with their propagated standard uncertainties (evaluated as described in Section III). In terms of selection accuracy, it can be observed that HoloLens 2 Head-Tracking demonstrates performance very close to 100%. Similar performance levels are achieved by HoloLens 2 eye-tracking (almost 98%), while the SSVEP-based NHMI based on HoloLens 2 and Unicorn Hybrid Black reaches approximately 74%. The propagated

TABLE I
SELECTION ACCURACY (%) FOR EACH INDIVIDUAL AND EACH NHMI IN TERMS OF MEAN AND PROPAGATED STANDARD UNCERTAINTY

Individual	Head-Tracking					Eye-Tracking					SSVEP BCI				
	C1	C2	C3	C4	C5	C1	C2	C3	C4	C5	C1	C2	C3	C4	C5
#1	100.0	100.0	100.0	100.0	100.0	100.0	100.0	100.0	100.0	100.0	62.5	75.0	25.0	87.5	87.5
#2	100.0	100.0	100.0	100.0	100.0	100.0	100.0	87.5	100.0	100.0	100.0	100.0	87.5	87.5	100.0
#3	100.0	100.0	100.0	100.0	100.0	100.0	100.0	100.0	100.0	100.0	12.5	62.5	75.0	50.0	62.5
#4	100.0	100.0	100.0	100.0	100.0	87.5	100.0	100.0	87.5	87.5	62.5	100.0	75.5	62.5	62.5
#5	100.0	100.0	100.0	100.0	100.0	87.5	100.0	100.0	100.0	100.0	100.0	50.0	62.5	25.0	12.5
#6	100.0	100.0	100.0	100.0	100.0	100.0	87.5	100.0	100.0	100.0	100.0	100.0	100.0	100.0	100.0
#7	100.0	100.0	100.0	100.0	100.0	100.0	100.0	100.0	100.0	100.0	87.5	87.5	87.5	75.0	87.5
#8	100.0	87.5	100.0	100.0	100.0	87.5	100.0	100.0	100.0	100.0	50.0	62.5	87.5	87.5	50.0
Average	99.7 ± 0.3					97.8 ± 0.7					73.8 ± 3.1				

TABLE II
ITR (bit/min) FOR EACH INDIVIDUAL AND EACH NHMI IN TERMS OF MEAN AND PROPAGATED STANDARD UNCERTAINTY

Individual	Head-Tracking					Eye-Tracking					SSVEP BCI				
	C1	C2	C3	C4	C5	C1	C2	C3	C4	C5	C1	C2	C3	C4	C5
#1	120.0	120.0	120.0	120.0	120.0	120.0	120.0	120.0	120.0	120.0	39.7	59.5	3.3	84.2	84.2
#2	120.0	120.0	120.0	120.0	120.0	120.0	120.0	84.2	120.0	120.0	120.0	120.0	84.2	84.2	120.0
#3	120.0	120.0	120.0	120.0	120.0	120.0	120.0	120.0	120.0	120.0	0.0	39.7	59.5	23.9	39.7
#4	120.0	120.0	120.0	120.0	120.0	84.2	120.0	120.0	84.2	120.0	39.7	120.0	59.5	39.7	39.7
#5	120.0	120.0	120.0	120.0	120.0	84.2	120.0	120.0	120.0	120.0	120.0	23.9	39.7	3.3	0.0
#6	120.0	120.0	120.0	120.0	120.0	120.0	84.2	120.0	120.0	120.0	120.0	120.0	120.0	120.0	120.0
#7	120.0	120.0	120.0	120.0	120.0	120.0	120.0	120.0	120.0	120.0	84.2	84.2	84.2	59.5	84.2
#8	120.0	84.2	120.0	120.0	120.0	84.2	120.0	120.0	120.0	120.0	23.9	39.7	84.2	84.2	23.9
Average	118.7 ± 1.1					112.2 ± 5.6					62.7 ± 18.7				

uncertainty follows the same trend, being lower for head-tracking compared with eye-tracking and SSVEP NHMIs.

The same considerations apply to the evaluation of ITR, where head-tracking shows values close to 119 bit/min (out of a maximum of 120 bit/min), while eye-tracking is around 112 bit/min and SSVEP–BCI approximately 63 bit/min, a value in line with the state of the art of SSVEP–BCI in XR environments [13].

B. Statistical Analysis and Discussion

To assess performance in terms of intra- and interindividual variabilities, further analyses were conducted using ANOVA and the F-test for each NHMI separately. In particular, intraindividual variability was assessed by comparing, for each NHMI, the five accuracy vectors (one for each acquisition cycle), each comprising the results from the eight individuals. Conversely, interindividual variability was assessed by comparing, again for each NHMI, the eight accuracy vectors (one for each individual), each comprising the results from the five acquisition cycles. The choice of this type of test is due to its specific capability to analyze data from two or more groups, to determine whether the means of the considered groups are significantly different from each other. The chosen confidence level was $\alpha = 0.05$. The outcomes of the tests indicated that head-tracking and eye-tracking show low levels of both intra- and interindividual variabilities. In contrast, the SSVEP-based NHMI exhibited high variability both intra- and inter-individually. This resulted in poor repeatability and reproducibility of the performance of the latter NHMI, attributable to the intrinsic variability of EEG signals both within and across individuals.

Furthermore, it was verified whether there exists a statistically significant difference in average performance between the three NHMIs (eye-tracking, head-tracking, and SSVEP). This verification was conducted through three Wilcoxon tests (eye-tracking versus head-tracking, eye-tracking versus SSVEP–BCI, and head-tracking versus SSVEP–BCI). This choice was made because the Wilcoxon test allows for robust pairwise comparisons, even when the sample size is relatively small [43]. In this case, the significance level $\alpha = 0.05$ was adjusted according to the Bonferroni correction for multiple comparisons [44], resulting in a new threshold of $\alpha = 0.05/3$. The results indicated that the performance achieved by the head-tracking and eye-tracking interfaces based on HoloLens 2 was significantly better than those produced by the SSVEP NHMI based on HoloLens 2 and Unicorn Hybrid Black. However, the test did not reveal sufficient statistical evidence to reject the null hypothesis concerning the differences between head- and eye-tracking. Overall, the proposed method has confirmed, through a quantitative approach and considering the equipment of the case study: 1) the robustness of head- and eye-tracking NHMIs and 2) the significant variability of SSVEPs.

Importantly, the generality of this approach allows for extending the performance assessment to interfaces that can be developed with different hardware and software components. This extension can lead to different outcomes regarding which interface is preferable for maximizing information transfer, since the average performance of these NHMIs is closely dependent on the available sensing system and recognition algorithms.

VI. CONCLUSION

This article presented a platform-independent method for assessing the information transfer performance of hands-free NHMIs in XR environments. Three different NHMIs were considered: eye-tracking, head-tracking, and BCIs based on SSVEPs. The proposed method is characterized by a high degree of generalizability, as it is suitable for any XR platform equipped with at least one of the considered interfaces. As a case study of the method's application, Microsoft HoloLens 2 and Unicorn Hybrid Black were chosen as the XR and BCI platforms, respectively. The experimental results for the case study at hand demonstrate higher selection accuracy for head- and eye-tracking, both close to 100%, compared with SSVEP-based NHMI (approximately 74%). Furthermore, statistical analysis of intra- and inter-individual variabilities revealed that head- and eye-tracking are characterized by greater repeatability and reproducibility. This was in line with expectations, as neural signals are generally characterized by considerable variability both within and among individuals. These findings indicate the potential scalability of head- and eye-tracking NHMIs based on HoloLens 2 for widespread use in XR environments, even in scenarios with tight requirements. Clearly, the choice of hardware and software was aimed at illustrating a case study. The proposed method can be extended to any NHMI, allowing the evaluation of performance for the specific components at hand. Overall, this study lays the groundwork for further advancements in human–machine interaction and XR technology. Future work will focus on further investigating the maximum limit of the ITR for eye- and head-tracking interfaces, considering a set of different acquisition times and accommodating a larger number of icons within the FoV of XR devices to contribute to the development of more robust and user-centric systems aligned with the principles of *Industry 5.0*. With the aim of conducting more in-depth analyses in terms of ITR, the proposed setup for the XR environment, consisting of eight digital icons, can be improved by adding more icons.

Acknowledgment

Leopoldo Angrisani, Mauro D'Arco, Egidio De Benedetto, Luigi Duraccio, and Fabrizio Lo Regio are with the Department of Electrical Engineering and Information Technology (DIETI), University of Naples Federico II, 80125 Naples, Italy (e-mail: egidio.debenedetto@unina.it).

Annarita Tedesco is with the Department of Public Health, University of Naples Federico II, 80138 Naples, Italy.

References

[1] M. Nardo, D. Forino, and T. Murino, "The evolution of man–machine interaction: The role of human in Industry 4.0 paradigm," *Prod. Manuf. Res.*, vol. 8, no. 1, pp. 20–34, Jan. 2020.

[2] D. Gorecky, M. Schmitt, M. Loskyll, and D. Zühlke, "Human-machine-interaction in the Industry 4.0 era," in *Proc. 12th IEEE Int. Conf. Ind. Informat. (INDIN)*, Jul. 2014, pp. 289–294.

[3] L. Giancardo et al., "Computer keyboard interaction as an indicator of early Parkinson's disease," *Sci. Rep.*, vol. 6, no. 1, p. 34468, Oct. 2016.

[4] A. D. Cheok, S. W. Fong, K. H. Goh, X. Yang, W. Liu, and F. Farzbiz, "Human pacman: A sensing-based mobile entertainment system with ubiquitous computing and tangible interaction," in *Proc. 2nd workshop Netw. Syst. support for games*, May 2003, pp. 106–117.

[5] C. Guo and E. Sharlin, "Exploring the use of tangible user interfaces for human-robot interaction: A comparative study," in *Proc. SIGCHI Conf. Human Factors Comput. Syst.*, Apr. 2008, pp. 121–130.

[6] *Industry 5.0*. Accessed: Jan. 13, 2024. [Online]. Available: https://research-and-innovation.ec.europa.eu/research-area/industrial-research-and-innovation/industry-50_en

[7] C. Falcao, A. C. Lemos, and M. Soares, "Evaluation of natural user interface: A usability study based on the leap motion device," *Proc. Manuf.*, vol. 3, pp. 5490–5495, Jan. 2015.

[8] K. Krafka et al., "Eye tracking for everyone," in *Proc. IEEE Conf. Comput. Vis. Pattern Recognit. (CVPR)*, Jun. 2016, pp. 2176–2184.

[9] A. Al-Rahayfeh and M. Faezipour, "Eye tracking and head movement detection: A state-of-art survey," *IEEE J. Transl. Eng. Health Med.*, vol. 1, 2013, Art. no. 2100212.

[10] Y. Wang, X. Gao, B. Hong, C. Jia, and S. Gao, "Brain–computer interfaces based on visual evoked potentials," *IEEE Eng. Med. Biol. Mag.*, vol. 27, no. 5, pp. 64–71, Sep. 2008.

[11] R. T. Azuma, "A survey of augmented reality," *Presence Teleoperators Virtual Environ.*, vol. 6, no. 4, pp. 355–385, 1997.

[12] P. Cipresso, I. A. C. Giglioli, M. A. Raya, and G. Riva, "The past, present, and future of virtual and augmented reality research: A network and cluster analysis of the literature," *Frontiers Psychol.*, vol. 9, p. 2086, Nov. 2018.

[13] L. Angrisani, P. Arpaia, E. De Benedetto, L. Duraccio, F. Lo Regio, and A. Tedesco, "Wearable brain–computer interfaces based on steady-state visually evoked potentials and augmented reality: A review," *IEEE Sensors J.*, vol. 23, no. 15, pp. 16501–16514, Jun. 2023.

[14] E. Pasqualotto et al., "Usability and workload of access technology for people with severe motor impairment: A comparison of brain–computer interfacing and eye tracking," *Neurorehabilitation Neural Repair*, vol. 29, no. 10, pp. 950–957, Nov. 2015.

[15] V. Paelke and J. Bulk, "Designing user-guidance for extendend reality interfaces in industrial environments," in *Human-Technology Interaction: Shaping the Future of Industrial User Interfaces*. Cham, Switzerland: Springer, 2022, pp. 173–198.

[16] A. Herur-Raman, N. D. Almeida, W. Greenleaf, D. Williams, A. Karshenas, and J. H. Sherman, "Next-generation simulation—Integrating extended reality technology into medical education," *Frontiers Virtual Reality*, vol. 2, Sep. 2021, Art. no. 693399.

[17] J. Blattgerste, P. Renner, and T. Pfeiffer, "Advantages of eye-gaze over head-gaze-based selection in virtual and augmented reality under varying field of views," in *Proc. Workshop Commun. Gaze Interact.*, 2018, pp. 1–9.

[18] A. L. Gardony, R. W. Lindeman, and T. T. Brunyé, "Eye-tracking for human-centered mixed reality: Promises and challenges," *Proc. SPIE*, vol. 11310, pp. 230–247, Feb. 2020.

[19] S. Lu, Y. P. Sanchez Perdomo, X. Jiang, and B. Zheng, "Integrating eye-tracking to augmented reality system for surgical training," *J. Med. Syst.*, vol. 44, no. 11, p. 192, Nov. 2020.

[20] O. Špakov, H. Istance, K.-J. Räihä, T. Viitanen, and H. Siirtola, "Eye gaze and head gaze in collaborative games," in *Proc. 11th ACM Symp. Eye Tracking Res. Appl.*, 2019, pp. 1–9.

[21] *Head-Gaze*. Accessed: Apr. 10, 2024. [Online]. Available: https://learn.microsoft.com/en-us/windows/mixed-reality/design/gaze-and-commit-head

[22] A. Kumar, S. Pundlik, E. Peli, and G. Luo, "Comparison of visual SLAM and IMU in tracking head movement outdoors," *Behav. Res. Methods*, vol. 55, no. 6, pp. 2787–2799, Aug. 2022.

[23] E. Murphy-Chutorian and M. M. Trivedi, "Head pose estimation and augmented reality tracking: An integrated system and evaluation for monitoring driver awareness," *IEEE Trans. Intell. Transp. Syst.*, vol. 11, no. 2, pp. 300–311, Jun. 2010.

[24] *Gaze and Commit—Mixed Reality Toolkit*. Accessed: Jan. 30, 2024. [Online]. Available: https://learn.microsoft.com/en-us/windows/mixed-reality/design/gaze-and-commit

[25] W. Hess, "Head-tracking techniques for virtual acoustics applications," *Audio Eng. Soc. Conv.*, vol. 133, pp. 916–930, Jan. 2012.

[26] A. Apicella et al., "Employment of domain adaptation techniques in SSVEP-based brain–computer interfaces," *IEEE Access*, vol. 11, pp. 36147–36157, 2023.

[27] L.-L. Zeng et al., "Neurobiological basis of head motion in brain imaging," *Proc. Nat. Acad. Sci. USA*, vol. 111, no. 16, pp. 6058–6062, Apr. 2014.

[28] E. Yin, Z. Zhou, J. Jiang, Y. Yu, and D. Hu, "A dynamically optimized SSVEP brain–computer interface (BCI) speller," *IEEE Trans. Biomed. Eng.*, vol. 62, no. 6, pp. 1447–1456, Jun. 2015.

[29] E. Yin, Z. Zhou, J. Jiang, F. Chen, Y. Liu, and D. Hu, "A novel hybrid BCI speller based on the incorporation of SSVEP into the P300 paradigm," *J. Neural Eng.*, vol. 10, no. 2, Apr. 2013, Art. no. 026012.

[30] E. Yin, Z. Zhou, J. Jiang, F. Chen, Y. Liu, and D. Hu, "A speedy hybrid BCI spelling approach combining P300 and SSVEP," *IEEE Trans. Biomed. Eng.*, vol. 61, no. 2, pp. 473–483, Feb. 2014.

[31] C. Jia, X. Gao, B. Hong, and S. Gao, “Frequency and phase mixed coding in SSVEP-based brain–computer interface,” *IEEE Trans. Biomed. Eng.*, vol. 58, no. 1, pp. 200–206, Jan. 2011.
[32] G. R. Müller-Putz, R. Scherer, C. Brauneis, and G. Pfurtscheller, “Steady-state visual evoked potential (SSVEP)-based communication: Impact of harmonic frequency components,” *J. Neural Eng.*, vol. 2, no. 4, pp. 123–130, Dec. 2005.
[33] C. S. Herrmann, “Human EEG responses to 1–100 Hz flicker: Resonance phenomena in visual cortex and their potential correlation to cognitive phenomena,” *Exp. Brain Res.*, vol. 137, nos. 3–4, pp. 346–353, 2001.
[34] L. Angrisani, P. Arpaia, A. Esposito, and N. Moccaldi, “A wearable brain–computer interface instrument for augmented reality-based inspection in Industry 4.0,” *IEEE Trans. Instrum. Meas.*, vol. 69, no. 4, pp. 1530–1539, Apr. 2020.
[35] P. Arpaia, S. Criscuolo, E. De Benedetto, N. Donato, and L. Duraccio, “A wearable AR-based BCI for robot control in ADHD treatment: Preliminary evaluation of adherence to therapy,” in *Proc. 15th Int. Conf. Adv. Technol., Syst. Services Telecommun. (TELSIKS)*, Oct. 2021, pp. 321–324.
[36] P. Arpaia, E. De Benedetto, N. Donato, L. Duraccio, and N. Moccaldi, “A wearable SSVEP BCI for AR-based, real-time monitoring applications,” in *Proc. IEEE Int. Symp. Med. Meas. Appl. (MeMeA)*, Jun. 2021, pp. 1–6.
[37] *Evaluation of Measurement Data—Guide to the Expression of Uncertainty in Measurement, JCGM 100:2008 GUM 1995 With Minor Corrections*, document JCGM 100:2008, BIPM, 2008.
[38] *Microsoft Hololens 2 Home*. Accessed: Nov. 28, 2023. [Online]. Available: https://www.microsoft.com/en-us/hololens
[39] *Unicorn Hybrid Black*. Accessed: Feb. 26, 2024. [Online]. Available: https://www.unicorn-bi.com/product/unicorn-hybrid-black/
[40] S. Negi and R. Mitra, “Fixation duration and the learning process: An eye tracking study with subtitled videos,” *J. Eye Movement Res.*, vol. 13, no. 6, pp. 1–15, Aug. 2020.
[41] J. Llanes-Jurado, J. Marín-Morales, J. Guixeres, and M. Alcañiz, “Development and calibration of an eye-tracking fixation identification algorithm for immersive virtual reality,” *Sensors*, vol. 20, no. 17, p. 4956, Sep. 2020.
[42] X. Chen, Y. Wang, S. Gao, T.-P. Jung, and X. Gao, “Filter bank canonical correlation analysis for implementing a high-speed SSVEP-based brain–computer interface,” *J. Neural Eng.*, vol. 12, no. 4, Aug. 2015, Art. no. 046008.
[43] D. J. Sheskin, *Handbook of Parametric and Nonparametric Statistical Procedures*. Boca Raton, FL, USA: CRC Press, 2003.
[44] R. A. Armstrong, “When to use the Bonferroni correction,” *Ophthalmic Physiological Opt.*, vol. 34, no. 5, pp. 502–508, 2014.

Leopoldo Angrisani (Fellow, IEEE) is a Full Professor of Electrical and Electronic Measurements with the Department of Electrical Engineering and Information Technology, University of Naples Federico II, Naples, Italy, where he is also the Chair of the Board of the Ph.D. Program, Information and Communication Technology for Health (ICTH). From 2016 to 2023, he was the Head of CeSMA, Center of Advanced Metrological and Technological Services, University of Naples Federico II. His research activity is currently focused on the Internet of Things and cyber-physical measurement systems, green soft-growing sensors, measurement sustainability, measurement uncertainty, measurements for Industry 4.0, communication systems, and networks test and measurement.

Dr. Angrisani is a Fellow Member of the IEEE Instrumentation and Measurement and Communications Societies, the Chair of the IEEE Instrumentation and Measurement Society Italy Chapter, the Honorary Chairperson of the First (M&N 2019) and Second (M&N 2022) edition of the IEEE International Symposium on Measurements and Networking, and the General Chairperson of the second edition (MetroInd4.0&IoT 2019) of the IEEE International Workshop on Metrology for Industry 4.0 and IoT 2019. He was one of the promoters of the TC-37 “Measurements and Networking” technical committee of the IEEE Instrumentation and Measurement Society and the General Chairperson of the first (M&N2011), second (M&N2013), third (M&N2015), and fourth editions (M&N2017) of the IEEE International Workshop on Measurements and Networking.

Mauro D’Arco (Senior Member, IEEE) received the M.Sc. degree in electronic engineering from the University of Salerno, Fisciano, Italy, in 1999, and the Ph.D. degree in electrotechnical engineering from the University of Naples Federico II, Naples, Italy, in 2003.

He is a Full Professor with the University of Naples Federico II. His current research interests are advanced signal processing techniques adopted in instrumentation and measurements’ applications, applied metrology for human–machine interfaces, measurement sustainability, and measurement uncertainty.

Egidio De Benedetto (Senior Member, IEEE) received the M.S. degree in materials engineering and the Ph.D. degree in information engineering from the University of Salento, Lecce, Italy, in 2006 and 2010, respectively.

He has been with the Institute of Microelectronics and Microsystems, National Research Council, Naples, Italy, from 2010 to 2012. From 2012 to 2019, he was with the University of Salento. Since 2019, he has been an Associate Professor with the Department of Electrical Engineering and Information Technology, University of Naples Federico II, Naples.

Luigi Duraccio (Member, IEEE) received the M.S. (cum laude) degree in electronic engineering from the University of Naples Federico II, Naples, Italy, in 2018, and the Ph.D. (cum laude) degree in metrology from the Polytechnic University of Turin, Turin, Italy, in 2023.

He is a Researcher with the Department of Electrical Engineering and Information Technology, University of Naples Federico II. His current research interests include metrology applied to digital transition of industry and healthcare, human–machine interaction, environmental sustainability, and cyber-physical measurement systems.

Fabrizio Lo Regio (Graduate Student Member, IEEE) received the M.S. (cum laude) degree in biomedical engineering from the University of Naples Federico II, Naples, Italy, in 2022, where he is currently pursuing the Ph.D. degree in information technology and electrical engineering.

His current research interests include applied metrology for neural interfaces, human–machine interaction, eXtended reality, quantum measurements, and telecommunications systems and networks.

Annarita Tedesco received the M.S. degree in telecommunication engineering from the University of Naples Federico II, Naples, Italy, in 2002, and the Ph.D. degree from the University of Bordeaux, Bordeaux, France, in 2022.

She is a Researcher with the Department of Public Health, University of Naples Federico II. Her current research interests include biomedical applications, monitoring systems, AR-based measurement systems, measurements for Healthcare 4.0, sensor networks, human–computer interaction, and brain–computer interface.

Open Access funding provided by ‘Università degli Studi di Napoli "Federico II"’ within the CRUI CARE Agreement